

1/ S -expansion study of spin waves in a two-dimensional Heisenberg antiferromagnet

Jun-ichi Igarashi

Faculty of Science, Ibaraki University, Mito, Ibaraki 310-8512, Japan

Tatsuya Nagao

Faculty of Engineering, Gunma University, Kiryu, Gunma 376-8515, Japan

(Dated: February 8, 2020)

Abstract

We study the effects of quantum fluctuations on excitation spectra in the two-dimensional Heisenberg antiferromagnet by means of the 1/ S expansion. We calculate the spin-wave dispersion and the transverse dynamical structure factor up to the second order of 1/ S in comparison with inelastic neutron scattering experiments. The spin-wave energy at momentum $(\pi, 0)$ is found to be about 2% smaller than that at $(\pi/2, \pi/2)$ due to the second-order correction. In addition, we study the dimensional crossover from two dimensions to one dimension by weakening exchange couplings in one direction. It is found that the second-order correction becomes large with approaching the quasi-one dimensional situation and makes the spin-wave energy approach to the des Cloizeaux-Pearson boundary for $S = 1/2$. The transverse dynamical structure factor is also calculated up to the second order of 1/ S . It is shown that the second-order correction gives rise to large intensities of three-spin-wave continuum in the quasi-one dimensional situation.

PACS numbers: 75.40.Gb, 75.10.Jm, 75.30.Ds

I. INTRODUCTION

The physics of low-dimensional spin systems has attracted much interest for past decades. Although the quantum fluctuation is expected to be large in two dimensions, there exist strong evidences that the quantum Heisenberg antiferromagnet (QHAF) with nearest-neighbor coupling in a square lattice exhibits the Néel long-range order at zero temperature.¹ Under the presence of the long-range order, the linear spin-wave (LSW) theory works rather well.^{2,3} A natural way to include quantum fluctuations is an expansion in terms of $1/S$, where S is the magnitude of spin, because the LSW theory is made up of a leading-order in the $1/S$ expansion. Such attempts have been done and turned out to be useful.^{4,5,6,7,8,9}

In our previous paper,⁵ basing on the Holstein-Primakoff transformation,¹⁰ we calculated corrections up to the second order of $1/S$ in various physical quantities such as the spin-wave dispersion, the sublattice magnetization, the perpendicular susceptibility, and the spin-stiffness constant. We also calculated the dynamical structure factors of the transverse and the longitudinal components up to the second order of $1/S$.⁶ At that time, however, available experimental data of inelastic neutron scattering (INS) were limited to the momentum transfer in a narrow region of the Brillouin zone (BZ). Therefore, our study was just a demonstration of usefulness of the $1/S$ expansion. Now that INS experiments provide us the information of the excitation spectra in the whole BZ, it may be interesting to calculate the excitation spectra in the whole BZ in comparison with recent experiments. We show that the second-order correction makes the spin wave energy at momentum $(\pi, 0)$ about 2% smaller than that at $(\pi/2, \pi/2)$. This difference is smaller than the value $7 \sim 9\%$ obtained by the series expansion^{11,12} and the Monte Carlo simulation.¹³ We have so far not been able to find why the $1/S$ expansion within the second order gives different results, since the higher-order corrections is expected to be quite small. Note that the spin-wave dispersion was recently measured by the INS experiment for $\text{Cu}(\text{DCOO})_2 \cdot 4\text{D}_2\text{O}$ (CFTD), revealing the 6% difference.^{14,15} This material is believed to be well described by the $S = 1/2$ Heisenberg model within the nearest-neighbor coupling.¹⁶ In addition to the spin-wave energy, we calculate the transverse dynamical structure factor up to the second order of $1/S$. It consists of the δ -function-like peak of one spin-wave excitation and the continuum of three spin-wave excitations. The second-order correction is found quite small in the spin-wave-peak intensity due to a cancellation of various second-order processes. The result is compared with

the recent experiment¹⁵ as well as other $1/S$ -expansion study¹⁷ based on the Dyson-Maleev transformation and the series expansion studies.^{11,12} In the three-spin-wave continuum, such a cancellation in the second-order processes is not severe, and the substantial intensities come out. This is consistent with our previous study⁶ and others.^{11,12,17}

Another purpose of this paper is to study the crossover behavior in the QHAF from two dimensions to one dimension with weakening exchange coupling in one direction. In purely one dimension, of course, the antiferromagnetic long-range order disappears due to quantum fluctuation and therefore the concept of spin waves breaks down. Carrying out the $1/S$ expansion, we demonstrate that the second-order corrections increase with approaching the quasi-one dimensional situation. The sublattice magnetization is shown to become small due to the second-order correction in the quasi-one dimensional situation. Interestingly, the spin-wave dispersion is found to approach to the curve known as the des Cloizaux-Pearson boundary in the $S = 1/2$ QHAF chain.¹⁸ At the same time, for the spin-wave peak in the transverse dynamical structure factor, the first-order correction makes the intensity decrease but the second-order correction makes it increase. In the quasi-one dimensional situation, both effects are nearly canceled out and the intensity is practically given by the zeroth-order value. The intensity of three-spin-wave continuum by the second-order correction increases and becomes comparable with the spin wave intensities in the quasi-one dimensional situation. This contrasts with the description of using spinon¹⁹ to describe the large intensity of the spectral continuum.

The present paper is organized as follows. In Sec. II, the Heisenberg Hamiltonian is expressed in terms of the $1/S$ -expansion. The Green's functions for spin waves are introduced in Sec. III. The sublattice magnetization is calculated with the help of the Green's functions in Sec. IV. The spin-wave dispersion is calculated in Sec. V, and the transverse dynamical structure factor is calculated in Sec. VI. Section VII is devoted to the concluding remarks.

II. HAMILTONIAN

We consider the Heisenberg Hamiltonian on the square lattice with directional anisotropy of exchange couplings:

$$H = J \sum_{\ell} \mathbf{S}_{\ell} \cdot \mathbf{S}_{\ell+\mathbf{a}} + J' \sum_{\ell} \mathbf{S}_{\ell} \cdot \mathbf{S}_{\ell+\mathbf{b}}, \quad (2.1)$$

where ℓ runs over all lattice sites and $\ell + \mathbf{a}$ and $\ell + \mathbf{b}$ indicate the nearest neighbors to the ℓ th site in the positive x and y directions, respectively. Quasi-one dimensional situations are realized by weakening the exchange coupling J' in the y direction.

Introducing the Holstein-Primakoff transformation,¹⁰ we express the spin operators in terms of boson annihilation operators a_i and b_j (and their Hermite conjugates),

$$S_i^z = S - a_i^\dagger a_i, \quad (2.2)$$

$$S_i^+ = (S_i^-)^\dagger = \sqrt{2S} f_i(S) a_i, \quad (2.3)$$

$$S_j^z = -S + b_j^\dagger b_j, \quad (2.4)$$

$$S_j^+ = (S_j^-)^\dagger = \sqrt{2S} b_j^\dagger f_j(S), \quad (2.5)$$

where

$$f_\ell(S) = \left(1 - \frac{n_\ell}{2S}\right)^{1/2} = 1 - \frac{1}{2} \frac{n_\ell}{2S} - \frac{1}{8} \left(\frac{n_\ell}{2S}\right)^2 + \dots \quad (2.6)$$

with $n_\ell = a_i^\dagger a_i$ and $b_j^\dagger b_j$. Indices i and j refer to sites on the "up" and "down" sublattices, respectively. Substituting Eqs. (2.2)-(2.5) into Eq. (2.1) we expand the Hamiltonian in powers of $1/S$ as

$$H = -S^2 N(J + J') + H_0 + H_1 + H_2 + \dots, \quad (2.7)$$

with N the number of lattice sites.

The leading term H_0 is expressed as

$$H_0 = JS \sum_i (2a_i^\dagger a_i + 2b_{i+\mathbf{a}}^\dagger b_{i+\mathbf{a}} + a_i^\dagger b_{i+\mathbf{a}} + a_i b_{i+\mathbf{a}}^\dagger + a_i^\dagger b_{i-\mathbf{a}}^\dagger + a_i^\dagger b_{i-\mathbf{a}}^\dagger) + J'S \sum_i (2a_i^\dagger a_i + 2b_{i+\mathbf{b}}^\dagger b_{i+\mathbf{b}} + a_i^\dagger b_{i+\mathbf{b}} + a_i b_{i+\mathbf{b}}^\dagger + a_i^\dagger b_{i-\mathbf{b}}^\dagger + a_i^\dagger b_{i-\mathbf{b}}^\dagger). \quad (2.8)$$

We diagonalize H_0 by rewriting the boson operators in the momentum space as

$$a_i = \left(\frac{2}{N}\right)^{1/2} \sum_{\mathbf{k}} a_{\mathbf{k}} \exp(i\mathbf{k} \cdot \mathbf{r}_i), \quad (2.9)$$

$$b_j = \left(\frac{2}{N}\right)^{1/2} \sum_{\mathbf{k}} b_{\mathbf{k}} \exp(i\mathbf{k} \cdot \mathbf{r}_j), \quad (2.10)$$

and by introducing the Bogoliubov transformation,

$$a_{\mathbf{k}}^\dagger = \ell_{\mathbf{k}} \alpha_{\mathbf{k}}^\dagger + m_{\mathbf{k}} \beta_{-\mathbf{k}}, \quad b_{-\mathbf{k}} = m_{\mathbf{k}} \alpha_{\mathbf{k}}^\dagger + \ell_{\mathbf{k}} \beta_{-\mathbf{k}}, \quad (2.11)$$

where

$$\ell_{\mathbf{k}} = \left[\frac{1 + \epsilon_{\mathbf{k}}}{2\epsilon_{\mathbf{k}}}\right]^{1/2}, \quad m_{\mathbf{k}} = -\text{sgn}(\gamma_{\mathbf{k}}) \left[\frac{1 - \epsilon_{\mathbf{k}}}{2\epsilon_{\mathbf{k}}}\right]^{1/2} \equiv -x_{\mathbf{k}} \ell_{\mathbf{k}}, \quad (2.12)$$

with

$$\epsilon_{\mathbf{k}} = (1 - \gamma_{\mathbf{k}}^2)^{1/2}, \quad (2.13)$$

$$\gamma_{\mathbf{k}} = (\cos k_x + \zeta \cos k_y) / (1 + \zeta), \quad (2.14)$$

$$\zeta = J'/J. \quad (2.15)$$

Momentum \mathbf{k} is defined in the first magnetic Brillouin zone (BZ). The $\text{sgn}(\gamma_{\mathbf{k}})$ denotes the sign of $\gamma_{\mathbf{k}}$, which is absorbed into the definition of $x_{\mathbf{k}}$. For the study of the isotropic exchange coupling ($\zeta = 1$), we have neglected this factor because $\gamma_{\mathbf{k}}$ is always positive in the first BZ. For the anisotropic coupling, however, this redefinition of $x_{\mathbf{k}}$ is necessary, because $\gamma_{\mathbf{k}}$ is negative in a certain region of the first BZ. After this transformation, we have

$$\begin{aligned} H_0 = & 2JS(1 + \zeta) \sum_{\mathbf{k}} (\epsilon_{\mathbf{k}} - 1) \\ & + 2JS(1 + \zeta) \sum_{\mathbf{k}} \epsilon_{\mathbf{k}} (\alpha_{\mathbf{k}}^\dagger \alpha_{\mathbf{k}} + \beta_{\mathbf{k}}^\dagger \beta_{\mathbf{k}}). \end{aligned} \quad (2.16)$$

This expression is the same as that for the isotropic coupling, except for the first factor $2JS(1 + \zeta)$.

The first-order term H_1 can be expressed in terms of spin-wave operators through the same procedure as above. The result for the anisotropic coupling is simply given by the previous expression in Ref. 5 with simply replacing JSz by $2JS(1 + \eta)$:

$$\begin{aligned} H_1 = & \frac{2JS(1 + \zeta)}{2S} A \sum_{\mathbf{k}} \epsilon_{\mathbf{k}} (\alpha_{\mathbf{k}}^\dagger \alpha_{\mathbf{k}} + \beta_{\mathbf{k}}^\dagger \beta_{\mathbf{k}}) \\ & + \frac{-2JS(1 + \zeta)}{2SN} \sum_{1234} \delta_{\mathbf{G}}(1 + 2 - 3 - 4) \ell_1 \ell_2 \ell_3 \ell_4 \\ & \times \left[\alpha_1^\dagger \alpha_2^\dagger \alpha_3 \alpha_4 B_{1234}^{(1)} + \beta_{-3}^\dagger \beta_{-4}^\dagger \beta_{-1} \beta_{-2} B_{1234}^{(2)} + 4 \alpha_1^\dagger \beta_{-4}^\dagger \beta_{-2} \alpha_3 B_{1234}^{(3)} \right. \\ & \left. + (2 \alpha_1^\dagger \beta_{-2} \alpha_3 \alpha_4 B_{1234}^{(4)} + 2 \beta_{-4}^\dagger \beta_{-1} \beta_{-2} \alpha_3 B_{1234}^{(5)} + \alpha_1^\dagger \alpha_2^\dagger \beta_{-3}^\dagger \beta_{-4}^\dagger B_{1234}^{(6)} + \text{H.c.}) \right], \end{aligned} \quad (2.17)$$

with

$$A = \frac{2}{N} \sum_{\mathbf{k}} (1 - \epsilon_{\mathbf{k}}). \quad (2.18)$$

Momenta $\mathbf{k}_1, \mathbf{k}_2, \mathbf{k}_3, \dots$ are abbreviated as $1, 2, 3, \dots$. The first term arises from setting the products of four boson operators into normal product forms with respect to spin-wave operators. The second term in eq. (2.17) represents the scattering of spin waves. The

Kronecker delta $\delta_{\mathbf{G}}(1+2-3-4)$ represents the conservation of momenta within a reciprocal lattice vector \mathbf{G} . The vertex functions $B^{(i)}$'s in a symmetric parameterization are the same as those given by Eqs. (2.16)-(2.20) in Ref. 5, so that they are omitted here.

The second-order term H_2 is composed of products of six boson operators. Writing it in a normal product form with respect to spin-wave operators, we have

$$H_2 = \frac{2JS(1+\zeta)}{(2S)^2} \sum_{\mathbf{k}} \left[C_1(\mathbf{k})(\alpha_{\mathbf{k}}^\dagger \alpha_{\mathbf{k}} + \beta_{\mathbf{k}}^\dagger \beta_{\mathbf{k}}) + C_2(\mathbf{k})(\alpha_{\mathbf{k}}^\dagger \beta_{-\mathbf{k}}^\dagger + \beta_{-\mathbf{k}} \alpha_{\mathbf{k}}) + \dots \right]. \quad (2.19)$$

Neglected terms are unnecessary for calculating corrections up to the second order. The explicit forms of $C_1(\mathbf{k})$ and $C_2(\mathbf{k})$, are given by Eqs. (2.22) and (2.23) in Ref. 5. Note that $C_1(\mathbf{k})$ and $C_2(\mathbf{k})$ diverge as $1/\epsilon_{\mathbf{k}}$ with $|\mathbf{k}| \rightarrow 0$.

III. GREEN'S FUNCTION

For systematically carrying out the $1/S$ -expansion, it is convenient to introduce the Green's functions for spin-waves,

$$G_{\alpha\alpha}(\mathbf{k}, t) = -i \langle T(\alpha_{\mathbf{k}}(t)\alpha_{\mathbf{k}}^\dagger(0)) \rangle, \quad (3.1)$$

$$G_{\alpha\beta}(\mathbf{k}, t) = -i \langle T(\alpha_{\mathbf{k}}(t)\beta_{-\mathbf{k}}(0)) \rangle, \quad (3.2)$$

$$G_{\beta\alpha}(\mathbf{k}, t) = -i \langle T(\beta_{-\mathbf{k}}^\dagger(t)\alpha_{\mathbf{k}}^\dagger(0)) \rangle, \quad (3.3)$$

$$G_{\beta\beta}(\mathbf{k}, t) = -i \langle T(\beta_{-\mathbf{k}}^\dagger(t)\beta_{-\mathbf{k}}(0)) \rangle, \quad (3.4)$$

where $\langle \dots \rangle$ denotes the average over the ground state, and T is the time-ordering operator.

In this paper, we measure energies in units of $2JS(1+\zeta)$. The unperturbed propagators corresponding to H_0 are given by

$$G_{\alpha\alpha}^0(\mathbf{k}, \omega) = [\omega - \epsilon_{\mathbf{k}} + i\delta]^{-1}, \quad (3.5)$$

$$G_{\alpha\beta}^0(\mathbf{k}, \omega) = G_{\beta\alpha}^0(\mathbf{k}, \omega) = 0, \quad (3.6)$$

$$G_{\beta\beta}^0(\mathbf{k}, \omega) = [-\omega - \epsilon_{\mathbf{k}} + i\delta]^{-1}. \quad (3.7)$$

The self-energy is defined by

$$G_{\mu\nu}(\mathbf{k}, \omega) = G_{\mu\nu}^0(\mathbf{k}, \omega) + \sum_{\mu'\nu'} G_{\mu\mu'}^0(\mathbf{k}, \omega) \Sigma_{\mu'\nu'}(\mathbf{k}, \omega) G_{\nu'\nu}(\mathbf{k}, \omega). \quad (3.8)$$

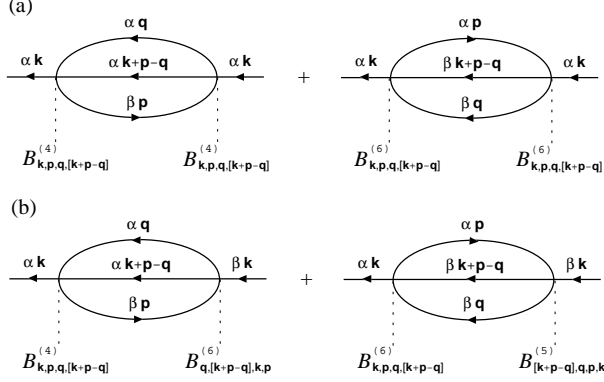


FIG. 1: Second-order diagrams for the self-energy, (a) $\Sigma_{\alpha\alpha}(\mathbf{k}, \omega)$ and (b) $\Sigma_{\alpha\beta}(\mathbf{k}, \omega)$. Solid lines represent the unperturbed Green's functions.

It is expanded in powers of $1/(2S)$,

$$\Sigma_{\mu\nu}(\mathbf{k}, \omega) = \frac{1}{2S} \Sigma_{\mu\nu}^{(1)}(\mathbf{k}, \omega) + \frac{1}{(2S)^2} \Sigma_{\mu\nu}^{(2)}(\mathbf{k}, \omega) + \dots . \quad (3.9)$$

From H_1 we have the first-order correction as

$$\Sigma_{\alpha\alpha}^{(1)}(\mathbf{k}, \omega) = \Sigma_{\beta\beta}^{(1)}(\mathbf{k}, \omega) = A\epsilon_{\mathbf{k}}, \quad \Sigma_{\alpha\beta}^{(1)}(\mathbf{k}, \omega) = \Sigma_{\beta\alpha}^{(1)}(\mathbf{k}, \omega) = 0. \quad (3.10)$$

The second-order term $\Sigma_{\mu\nu}^{(2)}(\mathbf{k}, \omega)$ is obtained from the second-order perturbation, whose diagrams are shown in Fig. 1. We obtain formally the same expression for the self-energy as in our previous paper:⁵

$$\begin{aligned} \Sigma_{\alpha\alpha}^{(2)}(\mathbf{k}, \omega) &= \Sigma_{\beta\beta}^{(2)}(-\mathbf{k}, -\omega) \\ &= C_1(\mathbf{k}) + \left(\frac{2}{N}\right)^2 \sum_{\mathbf{pq}} 2\ell_{\mathbf{k}}^2 \ell_{\mathbf{p}}^2 \ell_{\mathbf{q}}^2 \ell_{\mathbf{k}+\mathbf{p}-\mathbf{q}}^2 \\ &\quad \times \left[\frac{|B_{\mathbf{k},\mathbf{p},\mathbf{q},[\mathbf{k}+\mathbf{p}-\mathbf{q}]}^{(4)}|^2}{\omega - \epsilon_{\mathbf{p}} - \epsilon_{\mathbf{q}} - \epsilon_{\mathbf{k}+\mathbf{p}-\mathbf{q}} + i\delta} - \frac{|B_{\mathbf{k},\mathbf{p},\mathbf{q},[\mathbf{k}+\mathbf{p}-\mathbf{q}]}^{(6)}|^2}{\omega + \epsilon_{\mathbf{p}} + \epsilon_{\mathbf{q}} + \epsilon_{\mathbf{k}+\mathbf{p}-\mathbf{q}} - i\delta} \right], \end{aligned} \quad (3.11)$$

$$\begin{aligned} \Sigma_{\alpha\beta}^{(2)}(\mathbf{k}, \omega) &= \Sigma_{\beta\alpha}^{(2)}(-\mathbf{k}, -\omega) \\ &= C_2(\mathbf{k}) + \left(\frac{2}{N}\right)^2 \sum_{\mathbf{pq}} 2\ell_{\mathbf{k}}^2 \ell_{\mathbf{p}}^2 \ell_{\mathbf{q}}^2 \ell_{\mathbf{k}+\mathbf{p}-\mathbf{q}}^2 \text{sgn}(\gamma_{\mathbf{G}}) \\ &\quad \times B_{\mathbf{k},\mathbf{p},\mathbf{q},[\mathbf{k}+\mathbf{p}-\mathbf{q}]}^{(4)} B_{\mathbf{k},\mathbf{p},\mathbf{q},[\mathbf{k}+\mathbf{p}-\mathbf{q}]}^{(6)} \frac{2(\epsilon_{\mathbf{p}} + \epsilon_{\mathbf{q}} + \epsilon_{\mathbf{k}+\mathbf{p}-\mathbf{q}})}{\omega^2 - (\epsilon_{\mathbf{p}} + \epsilon_{\mathbf{q}} + \epsilon_{\mathbf{k}+\mathbf{p}-\mathbf{q}})^2 + i\delta}, \end{aligned} \quad (3.12)$$

where $\delta \rightarrow 0$, and $[\mathbf{k} + \mathbf{p} - \mathbf{q}]$ is the vector $\mathbf{k} + \mathbf{p} - \mathbf{q}$ reduced to the 1st BZ by a reciprocal vector \mathbf{G} . We have used the relations

$$\begin{aligned} B_{[\mathbf{k}+\mathbf{p}-\mathbf{q}],\mathbf{q},\mathbf{p},\mathbf{k}}^{(5)} &= \text{sgn}(\gamma_{\mathbf{G}}) B_{\mathbf{k},\mathbf{p},\mathbf{q},[\mathbf{k}+\mathbf{p}-\mathbf{q}]}^{(4)}, \\ B_{\mathbf{q},[\mathbf{k}+\mathbf{p}-\mathbf{q}],\mathbf{k},\mathbf{p}}^{(6)} &= \text{sgn}(\gamma_{\mathbf{G}}) B_{\mathbf{k},\mathbf{p},\mathbf{q},[\mathbf{k}+\mathbf{p}-\mathbf{q}]}^{(6)}. \end{aligned} \quad (3.13)$$

The terms divergent with $\mathbf{k} \rightarrow 0$ in $C_1(\mathbf{k})$ and $C_2(\mathbf{k})$ are canceled by the second-order perturbation terms in Eqs. (3.11) and (3.12). One can prove $\Sigma_{\mu\nu}^{(2)}(\mathbf{k} \rightarrow 0, \omega = 0) \rightarrow 0$ from these equations.

IV. SUBLATTICE MAGNETIZATION

Once the Green's function is known, the sublattice magnetization is calculated from the relation,

$$\begin{aligned} M &\equiv S - \langle a_i^\dagger a_i \rangle \\ &= S - \frac{2}{N} \sum_{\mathbf{k}} \lim_{\eta \rightarrow 0^+} \int_{-\infty}^{+\infty} \frac{d\omega}{2\pi} i e^{i\omega\eta} \left\{ \ell_{\mathbf{k}}^2 G_{\alpha\alpha}(\mathbf{k}, \omega) \right. \\ &\quad \left. + \ell_{\mathbf{k}} m_{\mathbf{k}} [G_{\alpha\beta}(\mathbf{k}, \omega) + G_{\beta\alpha}(\mathbf{k}, \omega)] + m_{\mathbf{k}}^2 G_{\beta\beta}(\mathbf{k}, \omega) \right\}, \end{aligned} \quad (4.1)$$

with $\eta \rightarrow 0^+$. After carrying out the integration with respect to ω , we obtain

$$M = S - \Delta S + \frac{M_2}{(2S)^2}, \quad (4.2)$$

with

$$\Delta S = \frac{2}{N} \sum_{\mathbf{k}} \frac{1}{2} (\epsilon_{\mathbf{k}}^{-1} - 1), \quad (4.3)$$

$$\begin{aligned} M_2 &= \frac{2}{N} \sum_{\mathbf{k}} \left\{ \frac{\ell_{\mathbf{k}} m_{\mathbf{k}}}{\epsilon_{\mathbf{k}}} \Sigma_{\alpha\beta}^{(2)}(\mathbf{k}, -\epsilon_{\mathbf{k}}) \right. \\ &\quad - \left(\frac{2}{N} \right)^2 \sum_{\mathbf{pq}} 2\ell_{\mathbf{k}}^2 \ell_{\mathbf{p}}^2 \ell_{\mathbf{q}}^2 \ell_{\mathbf{k}+\mathbf{p}-\mathbf{q}}^2 \left[\frac{(\ell_{\mathbf{k}}^2 + m_{\mathbf{k}}^2) |B_{\mathbf{k},\mathbf{p},\mathbf{q},[\mathbf{k}+\mathbf{p}-\mathbf{q}]}^{(6)}|^2}{(\epsilon_{\mathbf{k}} + \epsilon_{\mathbf{p}} + \epsilon_{\mathbf{q}} + \epsilon_{\mathbf{k}+\mathbf{p}-\mathbf{q}})^2} \right. \\ &\quad \left. \left. + \frac{2\ell_{\mathbf{k}} m_{\mathbf{k}} \text{sgn}(\gamma_{\mathbf{G}}) B_{\mathbf{k},\mathbf{p},\mathbf{q},[\mathbf{k}+\mathbf{p}-\mathbf{q}]}^{(4)} B_{\mathbf{k},\mathbf{p},\mathbf{q},[\mathbf{k}+\mathbf{p}-\mathbf{q}]}^{(6)}}{\epsilon_{\mathbf{k}}^2 - (\epsilon_{\mathbf{p}} + \epsilon_{\mathbf{q}} + \epsilon_{\mathbf{k}+\mathbf{p}-\mathbf{q}})^2} \right] \right\}. \end{aligned} \quad (4.4)$$

Here $[\mathbf{k} + \mathbf{p} - \mathbf{q}]$ was defined before, and $\mathbf{G} = \mathbf{k} + \mathbf{p} - \mathbf{q} - [\mathbf{k} + \mathbf{p} - \mathbf{q}]$. The zeroth-order correction ΔS represents the well-known “zero-point” reduction in the LSW theory.

Table I lists the values of ΔS and M_2 for several values of J'/J . For the isotropic coupling, we reproduce the values obtained previously. With decreasing values of J'/J , ΔS decrease first then increases slowly, while M_2 decreases monotonically and turns to be negative. Its absolute value is not large enough to destroy the long-range order even for $J'/J = 0.05$.

TABLE I: Sublattice magnetization

J'/J	1	0.5	0.1	0.05
ΔS	0.196	0.163	0.164	0.178
M_2	0.0035	0.001	-0.034	-0.067

V. SPIN-WAVE DISPERSION

Within the second order in $1/S$, the renormalized spin-wave energy $\tilde{\epsilon}_{\mathbf{k}}$ in units of $2JS(1+\zeta)$ is obtained from

$$\tilde{\epsilon}_{\mathbf{k}} = \epsilon_{\mathbf{k}} + \frac{1}{2S} A \epsilon_{\mathbf{k}} + \frac{1}{(2S)^2} \Sigma_{\alpha\alpha}^{(2)}(\mathbf{k}, \epsilon_{\mathbf{k}}). \quad (5.1)$$

From this equation, we define the renormalized spin-wave velocity V_x along the x direction by $V_x \equiv \lim_{k_x \rightarrow 0} 2JS(1+\zeta)\tilde{\epsilon}_{\mathbf{k}}/(\hbar k_x)$ with $k_y = 0$. Thus the renormalization factor is expressed as

$$Z_v \equiv \frac{V_x}{2JS(1+\zeta)^{1/2}} = 1 + \frac{v_1}{2S} + \frac{v_2}{(2S)^2}, \quad (5.2)$$

with $v_1 = A$ (Eq. (2.18)).

A. Isotropic case

Figure 2 shows the spin-wave energy $2JS(1+\zeta)\tilde{\epsilon}_{\mathbf{k}}$ as a function of momentum for the isotropic coupling ($\zeta = 1$) with $S = 1/2$, in comparison with the experimental data taken from the INS for $\text{Cu}(\text{DCOO})_2 \cdot 4\text{D}_2\text{O}$ (CFTD).^{14,15} Momentum is measured in units of (nearest neighbor distance)⁻¹. In the whole BZ, both the first and second order corrections make the spin-wave energy larger. The curve along the line $(0, 0) - (\pi, 0)$ has already been reported in our previous paper.⁵ The dispersion along $(\pi/2, \pi/2) - (\pi, 0)$ is completely flat within the first-order correction. The second-order correction makes the excitation energy at $(\pi, 0)$ about 2% smaller than the energy at $(\pi/2, \pi/2)$. Explicitly they are $\tilde{\epsilon}_{(\pi/2, \pi/2)} = 1.196$, $\tilde{\epsilon}_{(\pi, 0)} = 1.179$. A previous series expansion study predicted the energy difference about 7%,¹¹ and a recent study gave about 9% difference, that is, $\tilde{\epsilon}_{(\pi/2, \pi/2)} = 1.192$, $\tilde{\epsilon}_{(\pi, 0)} = 1.09$.¹² A Monte Carlo simulation has given $\tilde{\epsilon}_{(\pi/2, \pi/2)} = 1.195$, $\tilde{\epsilon}_{(\pi, 0)} = 1.08$.¹³ These values at $(\pi/2, \pi/2)$ agree well with our value, while the values at $(\pi, 0)$ is rather different from our estimate. The experimental data indicate that the excitation energy at $(\pi, 0)$ is 6% smaller

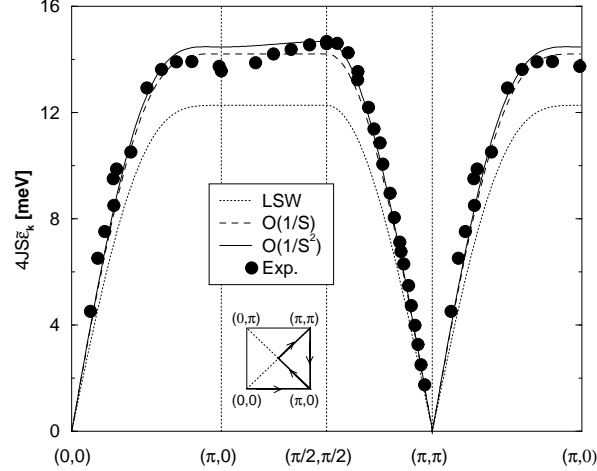


FIG. 2: Spin-wave energy as a function of momentum for the isotropic coupling ($\zeta = 1$). $S = 1/2$. The dotted, broken and solid lines represent the values calculated within the LSW theory, the first-order correction, and the second-order correction, respectively. Experimental data are taken from Ref. 15. Inset indicates high symmetry lines which momentum varies along.

TABLE II: Renormalization of spin-wave velocity

J'/J	1	0.5	0.1	0.05
v_1	0.158	0.132	0.154	0.167
v_2	0.021	0.053	0.131	0.153

than that at $(\pi/2, \pi/2)$.^{14,15}

B. Anisotropic case

Figure 3 shows the renormalized spin-wave energy as a function of momentum along $(0,0) - (\pi,0)$ for $\zeta < 1$. As the same as the isotropic coupling, both the first-order and the second-order corrections are found to be positive, making the energy larger. With decreasing values of ζ , the second-order correction particularly increases. In a quite small interchain coupling ($\zeta = 0.05$), the excitation energy seems approaching the *des Cloizeaux-Pearson boundary* in one dimension.¹⁸ As shown in Table II, the renormalization constant Z_v seems approaching $\pi/2$, corresponding to the value of the boundary.

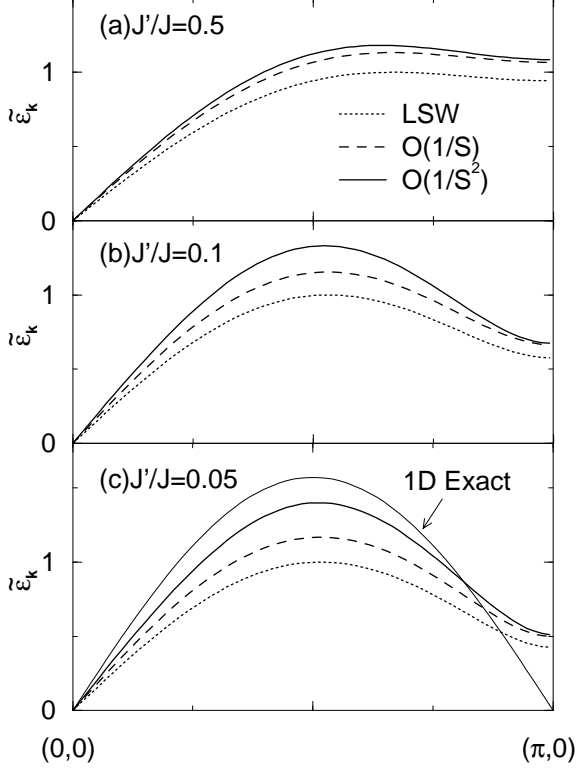


FIG. 3: Spin-wave energy as a function of momentum for anisotropic couplings, (a) $\zeta = 0.5$, (b) $\zeta = 0.1$, and (c) $\zeta = 0.05$. The dotted, broken and solid lines represent the values calculated within the LSW theory, the first-order correction, and the second-order correction, respectively. The thin solid line labelled “1D Exact” represents the des Cloizeaux-Pearson boundary.

VI. DYNAMICAL STRUCTURE FACTOR

The dynamical structure factor is an important quantity, since it is directly related to the INS spectra. We have already reported the expression within the second order of $1/S$ in the isotropic coupling situation.⁶ As is evident from the forms of H_0 and H_1 , the formulas for the anisotropic coupling are formally the same as those for the isotropic coupling.

We consider only the transverse component, which is defined by

$$S_{u(s)}^{+-}(\mathbf{k}, \omega) = \frac{1}{2\pi} \int dt e^{i\omega t} \langle Q_{u(s)}(\mathbf{k}, t) Q_{u(s)}(\mathbf{k}, 0)^\dagger \rangle, \quad (6.1)$$

where

$$Q_{u(s)}(\mathbf{k}) = S_a^+(\mathbf{k}) \pm S_b^+(\mathbf{k}), \quad (6.2)$$

with

$$S_a^+(\mathbf{k}) = [S_a^-(\mathbf{k})]^\dagger = \left(\frac{2}{N}\right)^{1/2} \sum_i S_i^+ \exp(-i\mathbf{k} \cdot \mathbf{r}_i), \quad (6.3)$$

$$S_b^+(\mathbf{k}) = [S_b^-(\mathbf{k})]^\dagger = \left(\frac{2}{N}\right)^{1/2} \sum_j S_j^+ \exp(-i\mathbf{k} \cdot \mathbf{r}_j). \quad (6.4)$$

We need the “uniform” and “staggered” parts because the momentum is defined inside the first BZ. They are labelled as the suffix “u” and “s”, and correspond to upper and lower signs in Eq. (6.2), respectively.

We start by introducing the operators,

$$Y_\alpha^+(\mathbf{k}) = [Y_\alpha^-(\mathbf{k})]^\dagger = [\ell_\mathbf{k} S_a^+(\mathbf{k}) - m_\mathbf{k} S_b^+(\mathbf{k})]/(2S)^{1/2}, \quad (6.5)$$

$$Y_\beta^+(\mathbf{k}) = [Y_\beta^-(\mathbf{k})]^\dagger = [-m_\mathbf{k} S_a^+(\mathbf{k}) + \ell_\mathbf{k} S_b^+(\mathbf{k})]/(2S)^{1/2}, \quad (6.6)$$

and the associated Green’s functions,

$$F_{\mu\nu}(\mathbf{k}, \omega) = -i \int_{-\infty}^{\infty} dt e^{i\omega t} \langle T[Y_\mu^+(\mathbf{k}, t) Y_\nu^-(\mathbf{k}, 0)] \rangle. \quad (6.7)$$

Then, with the help of the fluctuation-dissipation theorem, we have

$$\begin{aligned} S_{u(s)}^{+-}(\mathbf{k}, \omega) &= 2S(\ell_\mathbf{k} \pm m_\mathbf{k})^2 \left(-\frac{1}{\pi}\right) \\ &\times \text{Im}[F_{\alpha\alpha}(\mathbf{k}, \omega) \pm F_{\alpha\beta}(\mathbf{k}, \omega) \pm F_{\beta\alpha}(\mathbf{k}, \omega) + F_{\beta\beta}(\mathbf{k}, \omega)], \end{aligned} \quad (6.8)$$

where the upper (lower) signs correspond to the uniform (staggered) part.

For calculating $F_{\mu\nu}(\mathbf{k}, \omega)$, we expand the operator $Y_\mu^+(\mathbf{k})$ in terms of spin-wave operators with the help of the HP transformation and the Bogoliubov transformation. After lengthy calculations, we have

$$\begin{aligned} Y_\alpha^+(\mathbf{k}) &= D\alpha_\mathbf{k} - \frac{1}{2S} \frac{2}{N} \sum_{234} \delta_\mathbf{G}(\mathbf{k} + 2 - 3 - 4) \frac{1}{2} \ell_\mathbf{k} \ell_2 \ell_3 \ell_4 \\ &\times (M_{\mathbf{k}234}^{(1)} \beta_{-2} \alpha_3 \alpha_4 + M_{\mathbf{k}234}^{(2)} \alpha_2^\dagger \beta_{-3}^\dagger \beta_{-4}^\dagger + \dots), \end{aligned} \quad (6.9)$$

$$\begin{aligned} Y_\beta^+(\mathbf{k}) &= D\beta_{-\mathbf{k}}^\dagger \\ &- \frac{1}{2S} \frac{2}{N} \sum_{234} \delta_\mathbf{G}(\mathbf{k} + 2 - 3 - 4) \frac{1}{2} \ell_\mathbf{k} \ell_2 \ell_3 \ell_4 \text{sgn}(\gamma_\mathbf{G}) \\ &\times (M_{\mathbf{k}234}^{(2)} \beta_{-2} \alpha_3 \alpha_4 + M_{\mathbf{k}234}^{(1)} \alpha_2^\dagger \beta_{-3}^\dagger \beta_{-4}^\dagger + \dots), \end{aligned} \quad (6.10)$$

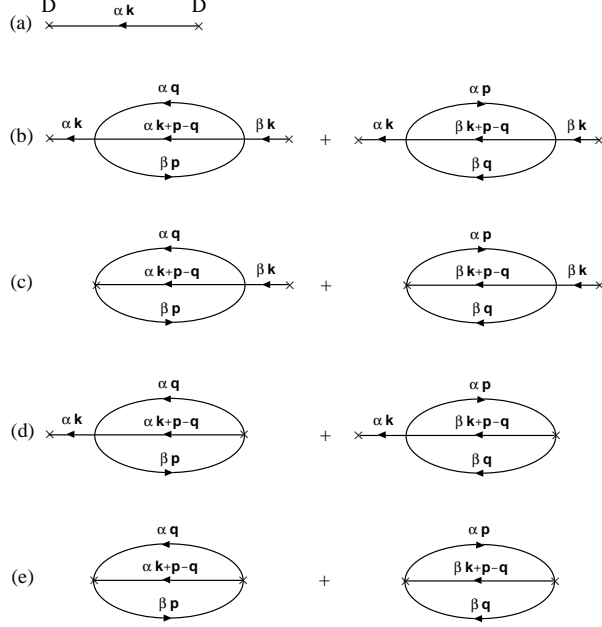


FIG. 4: Diagrams for $F_{\mu\nu}(\mathbf{k}, \omega)$. Solid lines represent the unperturbed Green's functions $G_{\mu\nu}^0(\mathbf{k}, \omega)$.

where

$$D = 1 - \frac{\Delta S}{2S} - \frac{1}{4} \frac{\Delta S(1 + 3\Delta S)}{(2S)^2}, \quad (6.11)$$

$$M_{\mathbf{k}234}^{(1)} = -x_2 + \text{sgn}(\gamma_{\mathbf{G}}) x_{\mathbf{k}} x_3 x_4, \quad (6.12)$$

$$M_{\mathbf{k}234}^{(2)} = x_3 x_4 - \text{sgn}(\gamma_{\mathbf{G}}) x_{\mathbf{k}} x_2. \quad (6.13)$$

with $\mathbf{G} = \mathbf{k} + 2 - 3 - 4$. The first-order and second-order corrections in Eq. (6.11) arises from setting four and six boson operators in the HP transformation into the normal product forms with spin-wave operators, respectively. Thereby, the second terms in Eqs. (6.9) and (6.10) are normally ordered. Note that $\text{sgn}(\gamma_{\mathbf{G}})$ arises from the phase difference in the definitions, Eqs. (6.3) and (6.4).

With the use of Eqs. (6.9) and (6.10), $F_{\mu\nu}(\mathbf{k}, \omega)$ is expanded up to the second order by the diagrams shown in Fig. 4. Explicitly, it is given by

$$\begin{aligned} F_{\mu\nu}(\mathbf{k}, \omega) = & D^2 G_{\mu\nu}^0(\mathbf{k}, \omega) \delta_{\mu\nu} + G_{\mu\mu}^0(\mathbf{k}, \omega) \frac{1}{(2S)^2} \Sigma_{\mu\nu}^{(2)}(\mathbf{k}, \omega) G_{\nu\nu}^0(\mathbf{k}, \omega) \\ & + I_{\mu\nu}(\mathbf{k}, \omega) G_{\nu\nu}^0(\mathbf{k}, \omega) + G_{\mu\mu}^0(\mathbf{k}, \omega) \tilde{I}_{\mu\nu}(\mathbf{k}, \omega) + J_{\mu\nu}(\mathbf{k}, \omega), \end{aligned} \quad (6.14)$$

where each term in Eq. (6.14) corresponds to the diagrams (a), (b), (c), (d), and (e), respectively. Explicit expressions for $I_{\mu\nu}(\mathbf{k}, \omega)$, $\tilde{I}_{\mu\nu}(\mathbf{k}, \omega)$, and $J_{\mu\nu}(\mathbf{k}, \omega)$ are given by Eqs. (4.5)-(4.22) in Ref. 5.

The dynamical structure factor is obtained by substituting Eq. (6.14) into Eq. (6.8). It consists of the δ -function-like peak of the one spin-wave excitation and the continuum of three spin-wave excitations:

$$S_{u(s)}^{+-}(\mathbf{k}, \omega) = \rho_{u(s)}^{(1)}(\mathbf{k})\delta(\omega - \epsilon_{\mathbf{k}}) + \rho_{u(s)}^{(2)}(\mathbf{k}, \omega). \quad (6.15)$$

For the term of one spin-wave excitation, the bare energy $\epsilon_{\mathbf{k}}$ is to be replaced by the renormalized value $\tilde{\epsilon}_{\mathbf{k}}$ given by Eq. (5.1). However, the spectral weight $\rho^{(1)}(\mathbf{k})$ within the second order of $1/S$ is safely evaluated by putting $\omega = \epsilon_{\mathbf{k}}$ in Eq. (6.14). It is expressed as

$$\rho_{u(s)}^{(1)}(\mathbf{k}) = 2S(\ell_{\mathbf{k}} \pm m_{\mathbf{k}})^2 \left(1 + \frac{d_{u(s),1}}{2S} + \frac{d_{u(s),2}}{(2S)^2} \right), \quad (6.16)$$

with

$$d_{u(s),1} = -2\Delta S, \quad (6.17)$$

$$\begin{aligned} d_{u(s),2} &= -\frac{1}{2}\Delta S(1 + \Delta S) \mp \frac{1}{\epsilon_{\mathbf{k}}}\Sigma_{\alpha\beta}^{(2)}(\mathbf{k}, \epsilon_{\mathbf{k}}) \\ &+ \left(\frac{2}{N} \right)^2 \sum_{\mathbf{pq}} 2\ell_{\mathbf{k}}^2 \ell_{\mathbf{p}}^2 \ell_{\mathbf{q}}^2 \ell_{\mathbf{k}+\mathbf{p}-\mathbf{q}}^2 \\ &\times \left[\frac{-|B_{\mathbf{k},\mathbf{p},\mathbf{q},[\mathbf{k}+\mathbf{p}-\mathbf{q}]}^{(4)}|^2}{(\epsilon_{\mathbf{k}} - \epsilon_{\mathbf{p}} - \epsilon_{\mathbf{q}} - \epsilon_{\mathbf{k}+\mathbf{p}-\mathbf{q}})^2} + \frac{|B_{\mathbf{k},\mathbf{p},\mathbf{q},[\mathbf{k}+\mathbf{p}-\mathbf{q}]}^{(6)}|^2}{(\epsilon_{\mathbf{k}} + \epsilon_{\mathbf{p}} + \epsilon_{\mathbf{q}} + \epsilon_{\mathbf{k}+\mathbf{p}-\mathbf{q}})^2} \right] \\ &+ \left(\frac{2}{N} \right)^2 \sum_{\mathbf{pq}} 2\ell_{\mathbf{k}}^2 \ell_{\mathbf{p}}^2 \ell_{\mathbf{q}}^2 \ell_{\mathbf{k}+\mathbf{p}-\mathbf{q}}^2 (M_{\mathbf{k},\mathbf{p},\mathbf{q},[\mathbf{k}+\mathbf{p}-\mathbf{q}]}^{(1)} \pm \text{sgn}(\gamma_{\mathbf{G}})M_{\mathbf{k},\mathbf{p},\mathbf{q},[\mathbf{k}+\mathbf{p}-\mathbf{q}]}^{(2)}) \\ &\times \left[\frac{B_{\mathbf{k},\mathbf{p},\mathbf{q},[\mathbf{k}+\mathbf{p}-\mathbf{q}]}^{(4)}}{(\epsilon_{\mathbf{k}} - \epsilon_{\mathbf{p}} - \epsilon_{\mathbf{q}} - \epsilon_{\mathbf{k}+\mathbf{p}-\mathbf{q}})} \mp \frac{\text{sgn}(\gamma_{\mathbf{G}})B_{\mathbf{k},\mathbf{p},\mathbf{q},[\mathbf{k}+\mathbf{p}-\mathbf{q}]}^{(6)}}{\epsilon_{\mathbf{k}} + \epsilon_{\mathbf{p}} + \epsilon_{\mathbf{q}} + \epsilon_{\mathbf{k}+\mathbf{p}-\mathbf{q}}} \right]. \end{aligned} \quad (6.18)$$

The upper (lower) signs correspond to the uniform (staggered) part. The first-order correction Eq. (6.17) arises from the first term of Eq. (6.14). In the second-order correction given by Eq. (6.18), the first term arises from the first term of Eq. (6.14), and the second term arises from the second term of Eq. (6.14),

$$G_{\alpha\alpha}^0(\mathbf{k}, \omega) \frac{1}{(2S)^2} \Sigma_{\alpha\beta}^{(2)}(\mathbf{k}, \omega) G_{\beta\beta}^0(\mathbf{k}, \omega) + G_{\beta\beta}^0(\mathbf{k}, \omega) \frac{1}{(2S)^2} \Sigma_{\beta\alpha}^{(2)}(\mathbf{k}, \omega) G_{\alpha\alpha}^0(\mathbf{k}, \omega).$$

The third term of Eq. (6.18) is equivalent to

$$\frac{1}{(2S)^2} \frac{\partial \Sigma_{\alpha\alpha}^{(2)}(\mathbf{k}, \omega)}{\partial \omega} \Bigg|_{\omega=\epsilon_{\mathbf{k}}},$$

and arises from the second term of Eq. (6.14),

$$G_{\alpha\alpha}^0(\mathbf{k}, \omega) \frac{1}{(2S)^2} \Sigma_{\alpha\alpha}^{(2)}(\mathbf{k}, \omega) G_{\alpha\alpha}^0(\mathbf{k}, \omega).$$

This is related to the second-order correction to the residue of the spin-wave pole in $G_{\alpha\alpha}(\mathbf{k}, \omega)$,

$$\frac{1}{1 - \frac{1}{(2S)^2} \frac{\partial \Sigma_{\alpha\alpha}^{(2)}(\mathbf{k}, \omega)}{\partial \omega} \Big|_{\omega=\epsilon_{\mathbf{k}}}} \approx 1 + \frac{1}{(2S)^2} \frac{\partial \Sigma_{\alpha\alpha}^{(2)}(\mathbf{k}, \omega)}{\partial \omega} \Big|_{\omega=\epsilon_{\mathbf{k}}}.$$

The fourth term arises from the third and fourth terms of Eq. (6.14),

$$I_{\mu\nu}(\mathbf{k}, \omega) G_{\nu\nu}^0(\mathbf{k}, \omega) + G_{\mu\mu}^0(\mathbf{k}, \omega) \tilde{I}_{\mu\nu}(\mathbf{k}, \omega).$$

No contribution arises from the last term of Eq. (6.14), $J_{\mu\nu}(\mathbf{k}, \omega)$. Note that the main momentum dependence around $\mathbf{k} = (0, 0)$ arises from the prefactors, $(\ell_{\mathbf{k}} + m_{\mathbf{k}})^2 \propto \epsilon_{\mathbf{k}}$ and $(\ell_{\mathbf{k}} - m_{\mathbf{k}})^2 \propto 1/\epsilon_{\mathbf{k}}$.

The three-spin-wave continuum arises only from the second-order corrections. Note that the first term of Eq. (6.14) has no contribution. After careful evaluation of other terms in Eq. (6.14), we obtain

$$\begin{aligned} \rho_{u(s)}^{(2)}(\mathbf{k}, \omega) &= 2S(\ell_{\mathbf{k}} \pm m_{\mathbf{k}})^2 \frac{1}{(2S)^2} \left(\frac{2}{N} \right)^2 \sum_{\mathbf{pq}} \delta(\omega - \epsilon_{\mathbf{p}} - \epsilon_{\mathbf{q}} - \epsilon_{\mathbf{k+p-q}}) \\ &\times \frac{1}{2} \ell_{\mathbf{k}}^2 \ell_{\mathbf{p}}^2 \ell_{\mathbf{q}}^2 \ell_{\mathbf{k+p-q}}^2 \left[M_{\mathbf{k}, \mathbf{p}, \mathbf{q}, [\mathbf{k+p-q}]}^{(1)} \pm \text{sgn}(\gamma_{\mathbf{G}}) M_{\mathbf{k}, \mathbf{p}, \mathbf{q}, [\mathbf{k+p-q}]}^{(2)} \right. \\ &\left. - \frac{2B_{\mathbf{k}, \mathbf{p}, \mathbf{q}, [\mathbf{k+p-q}]}^{(4)}}{\epsilon_{\mathbf{k}} - \epsilon_{\mathbf{p}} - \epsilon_{\mathbf{q}} - \epsilon_{\mathbf{k+p-q}}} \mp \frac{2\text{sgn}(\gamma_{\mathbf{G}}) B_{\mathbf{k}, \mathbf{p}, \mathbf{q}, [\mathbf{k+p-q}]}^{(6)}}{\epsilon_{\mathbf{k}} + \epsilon_{\mathbf{p}} + \epsilon_{\mathbf{q}} + \epsilon_{\mathbf{k+p-q}}} \right]^2. \end{aligned} \quad (6.19)$$

The spectral shape may be modified by the renormalization of spin-wave energies and by taking account of scattering spin waves due to mutual interaction, which terms are present in H_1 . Therefore, it may be difficult to determine the spectral shape in a consistent way with the $1/S$ expansion. However, the total intensity, which is given by

$$I_{u(s)}^{(2)}(\mathbf{k}) = \int_0^\infty d\omega \rho_{u(s)}^{(2)}(\mathbf{k}, \omega), \quad (6.20)$$

may be safely evaluated from Eq. (6.19). Note that around $\mathbf{k} = (0, 0)$

$$M_{\mathbf{k}, \mathbf{p}, \mathbf{q}, [\mathbf{k+p-q}]}^{(1)} \pm \text{sgn}(\gamma_{\mathbf{G}}) M_{\mathbf{k}, \mathbf{p}, \mathbf{q}, [\mathbf{k+p-q}]}^{(2)} \propto \epsilon_{\mathbf{k}}, \quad (6.21)$$

$$\begin{aligned} -\frac{B_{\mathbf{k}, \mathbf{p}, \mathbf{q}, [\mathbf{k+p-q}]}^{(4)}}{\epsilon_{\mathbf{k}} - \epsilon_{\mathbf{p}} - \epsilon_{\mathbf{q}} - \epsilon_{\mathbf{k+p-q}}} &\mp \frac{\text{sgn}(\gamma_{\mathbf{G}}) B_{\mathbf{k}, \mathbf{p}, \mathbf{q}, [\mathbf{k+p-q}]}^{(6)}}{\epsilon_{\mathbf{k}} + \epsilon_{\mathbf{p}} + \epsilon_{\mathbf{q}} + \epsilon_{\mathbf{k+p-q}}} \\ &\approx \frac{B_{\mathbf{k}, \mathbf{p}, \mathbf{q}, [\mathbf{k+p-q}]}^{(4)} \mp \text{sgn}(\gamma_{\mathbf{G}}) B_{\mathbf{k}, \mathbf{p}, \mathbf{q}, [\mathbf{k+p-q}]}^{(6)}}{\epsilon_{\mathbf{p}} + \epsilon_{\mathbf{q}} + \epsilon_{\mathbf{k+p-q}}} \propto \epsilon_{\mathbf{k}}, \end{aligned} \quad (6.22)$$

and $(\ell_{\mathbf{k}} + m_{\mathbf{k}})^2 \ell_{\mathbf{k}}^2 \propto \text{const.}$, $(\ell_{\mathbf{k}} - m_{\mathbf{k}})^2 \ell_{\mathbf{k}}^2 \propto 1/\epsilon_{\mathbf{k}}^2$, we notice the dependences around $\mathbf{k} = (0, 0)$ as $I_u^{(2)}(\mathbf{k}) \propto \epsilon_{\mathbf{k}}^2$, $I_s^{(2)}(\mathbf{k}) \propto \text{const.}$

A. Isotropic case

Figure 5 shows the spin-wave-peak intensity and the intensity of three-spin-wave continuum as a function of momentum along high-symmetry lines for $S = 1/2$. Using the extended zone scheme, we assign the staggered part for line $(0, 0) - (\pi/2, \pi/2)$ to the values for line $(\pi, \pi) - (\pi/2, \pi/2)$ and also the staggered part for line $(0, 0) - (\pi, 0)$ to the values for line $(\pi, \pi) - (\pi, 0)$. The uniform part is assigned inside the first BZ. At the zone boundary of the reduced BZ, the uniform and staggered parts coincide with each other. The second-order corrections to the spin-wave-peak intensity becomes one order of magnitude smaller than the first-order correction, due to a cancellation among contributions of four terms in Eq. (6.18). The intensity is almost determined within the first-order correction. Thus the correction relative to the zero-th order value is independent of momentum. We obtain around $\mathbf{k} = (0, 0)$,

$$\rho_u^{(1)}(\mathbf{k}) = 0.215|\mathbf{k}|, \quad \rho_s^{(1)}(\mathbf{k}) = 1.72/|\mathbf{k}| \quad (S = 1/2). \quad (6.23)$$

These values should be compared with the $1/S$ -expansion analysis based on the Dyson-Maleev transformation,¹⁷ 0.202 and 1.86. A series expansion analysis by Singh²⁰ gives the values, 0.246 and 2.10, while a recent analysis by Zheng *et al.*¹² gives the values, 0.216 and 1.86.

The small second-order correction to $\rho_{u(s)}^{(1)}(\mathbf{k})$ does not necessarily mean small three-spin-wave continuum. At the zone boundary $(\pi, 0)$, for example, we have $I^{(2)}(\pi, 0) = 0.143$ in addition to $\rho^{(1)}(\pi, 0) = 0.618$. Such a considerable intensity of three spin-wave continuum has been predicted in our previous paper⁶ and others.^{12,17} It varies as proportional to $\epsilon_{\mathbf{k}}^2$ at the zone center, and converges to a constant value at (π, π) .

B. Anisotropic case

Figure 6 shows the spin-wave-peak intensity and the intensity of three-spin-wave continuum along the symmetry line $(0, 0) - (\pi, 0)$ for several anisotropic couplings. $S = 1/2$.

The spin-wave-peak intensity is reduced by the first-order correction, but is increased by

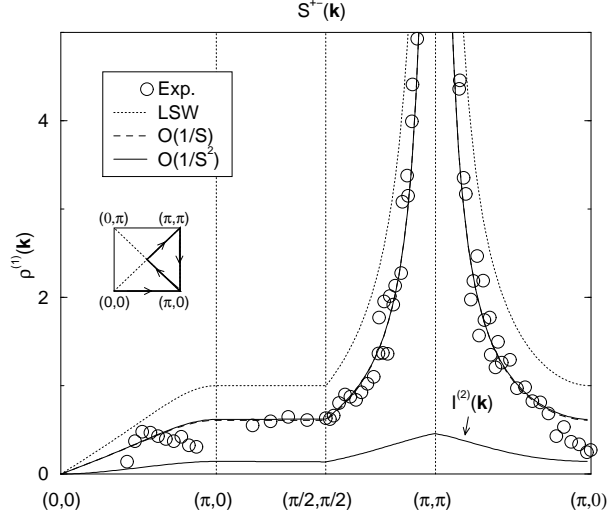


FIG. 5: Transverse dynamical structure factor as a function of momentum for the isotropic coupling. $S = 1/2$. The dotted, broken and solid lines represent the intensity of one spin-wave excitation calculated within the LSW theory, the first-order correction, and the second-order correction, respectively. Thin solid line represents the intensity of three spin-wave excitations. Experimental data are taken from Ref. 15. Inset indicates high symmetry lines which momentum varies along.

the second-order correction. Note that, although the residue of the spin-wave pole in the Green's function is reduced by the self-energy, the other terms of the second-order correction work to increase the intensity. The second-order correction increases with decreasing values of J'/J . In the quasi-one dimensional situation, the second-order correction nearly cancels the first-order correction, thus the intensity is almost given by the zeroth-order term (Fig. 6(c) and (f)).

The intensity of three-spin-wave continuum increases with decreasing values of J'/J . It reaches nearly the same order of magnitude of the spin-wave-peak intensity in the quasi-one dimensional situation. Such large intensities of continuum spectra have been observed in the recent INS experiments on the quasi-one dimensional QHAF such as KCuF_3 ²¹ and $\text{BaCu}_2\text{Si}_2\text{O}_7$.²²

VII. CONCLUDING REMARKS

We have systematically carried out the $1/S$ expansion up to the second order on the basis of the HP transformation in the two-dimensional QHAF. We have calculated the spin-wave

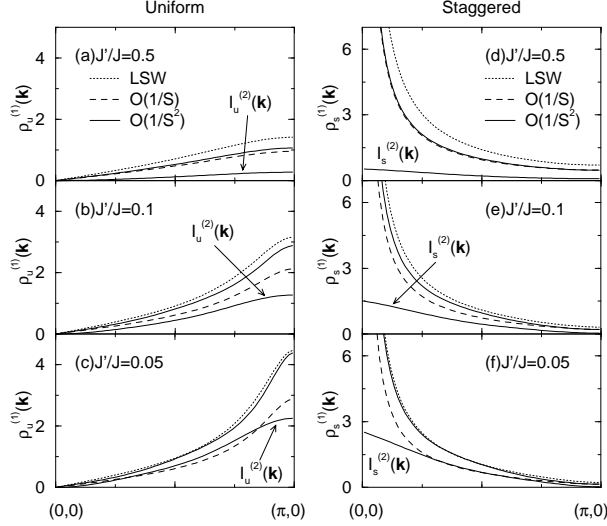


FIG. 6: Transverse dynamical structure factor as a function of momentum along the symmetric line $(0, 0) - (\pi, 0)$ for anisotropic couplings; (a) $J'/J = 0.5$, (b) $J'/J = 0.1$, and (c) $J'/J = 0.05$. $S = 1/2$. The dotted, broken and solid lines represent the spin-wave-peak intensity calculated within the LSW theory, the first-order correction, and the second-order correction, respectively. The thin solid line represents the three-spin-wave continuum intensity.

energy in the whole BZ, in comparison with the recent INS experiment for CFTD.^{14,15} We have found that the spin-wave energy at $(\pi, 0)$ is about 2% smaller than that at $(\pi/2, \pi/2)$ due to the second-order correction. This is a correct tendency, but the value is somewhat smaller than the experimental value 6% and other theoretical estimates 7 – 9%.^{11,12,13} We have so far not been able to find the reason for the difference, since the corrections higher than the second order of $1/S$ is expected to be quite small. We have also calculated the transverse dynamical structure factor. The second-order correction is found extremely small in the one-spin-wave-peak intensity due to the cancellation in the second-order terms, while it gives rise to substantial intensities of three-spin-wave continuum. This is consistent with previous studies.^{6,11,12,17}

The second-order correction is expected to become more important in quasi-one dimensional systems. We have studied the crossover from two dimensions to one dimension by weakening the exchange coupling in one direction. All formulas are found formally the same as those for the isotropic coupling with replacing JSz by $2JS(1 + \zeta)$. It is found that the excitation energy is pushed up by the first-order and second-order corrections. With approaching the quasi-one dimensional situation, the corrections make the excitation energy

close to the des Cloizeaux-Pearson boundary in the one-dimensional QHAF for $S = 1/2$. In the transverse dynamical structure factor, the spin-wave-peak intensity is reduced by the first-order correction, but is increased by the second-order correction. The latter nearly cancels the former in the quasi-one dimensional situation, thereby the peak intensity is almost determined by the zeroth-order value. The intensity of three-spin-wave continuum is found to reach nearly the same order of the spin-wave-peak intensity.

Recently, INS experiments have been carried out at low temperatures in the quasi-one dimensional systems such as KCuF_3 ²¹ and $\text{BaCu}_2\text{Si}_2\text{O}_7$,²² and large broad spectra have been observed in addition to a peak in the transverse dynamical structure factors. This behavior as well as the behavior of the longitudinal component have been analyzed by the chain-mean-field and random phase approximation.^{23,24} It may be interesting to analyze these data in terms of the $1/S$ expansion by starting from a detailed three-dimensional model with directional anisotropy.

Acknowledgments

J.I. thanks MPI-PKS at Dresden for hospitality during his stay, where this work started. This work was partially supported by a Grant-in-Aid for Scientific Research from the Ministry of Education, Science, Sports and Culture, Japan.

¹ S. Chakravarty, B. I. Halperin, and D. R. Nelson, Phys. Rev. B **39**, 2344 (1989).

² P. W. Anderson, Phys. Rev. **86**, 694 (1952).

³ R. Kubo, Phys. Rev. **87**, 568 (1952).

⁴ T. Oguchi, Phys. Rev. **117**, 117 (1960).

⁵ J. Igarashi, Phys. Rev. B **46**, 10763 (1992).

⁶ J. Igarashi, J. Phys.: Codens. Matter **4**, 10265 (1992).

⁷ J. Igarashi, J. Phys. Soc. Jpn. **62**, 4449 (1993).

⁸ C. M. Canali, S. M. Girvin, and M. Wallin, Phys. Rev. B **45**, R10131 (1992).

⁹ C. J. Hamer, W. Zheng, and P. Arndt, Phys. Rev. B **46**, 6276 (1992).

¹⁰ T. Holstein and H. Primakoff, Phys. Rev. **58**, 1098 (1940).

¹¹ R. R. P. Singh and M. P. Gelfand, Phys. Rev. B. **52**, R15695 (1995).

¹² W. Zheng, J. Oitmaa, and C. J. Hamer, cond-mat/0412184.

¹³ A. W. Sandvik and R. R. P. Singh, Phys. Rev. Lett. **86**, 528 (2001).

¹⁴ H. M. Rønnow, D. F. McMorrow, R. Coldea, A. Harrison, I. D. Youngson, T. G. Perring, G. Aeppli, O. Syljuåsen, K. Lefmann, and C. Rischel, Phys. Rev. Lett. **87**, 037202 (2001).

¹⁵ N. B. Christensen, D. F. McMorrow, H. M. Rønnow, A. Harrison, T. G. Perring, and R. Coldea, J. Mag. Magne. Mater. **272-276**, 896 (2004).

¹⁶ For La_2CuO_4 , the spin-wave energy at $(\pi, 0)$ is observed to be about 15% *larger* than at $(\pi/2, \pi/2)$ ²⁵. This tendency is opposite to the CFTD. In the picture of the half-filled Hubbard model, t/U in La_2CuO_4 is considered larger than in CFTD. Therefore, the difference might be understood by the effect of the next-nearest neighbor exchange coupling and/or ring exchange couplings.

¹⁷ C. M. Canali and M. Wallin, Phys. Rev. B **48**, 3264 (1993).

¹⁸ J. des Cloizeaux and J. J. Pearson, Phys. Rev. **128**, 2131 (1962).

¹⁹ C. M. Ho, V. N. Muthukumar, M. Ogata, and P. W. Anderson, Phys. Rev. Lett. **86**, 1626 (2001).

²⁰ R. R. P. Singh, Phys. Rev. B. **47**, R12337 (1993).

²¹ B. Lake, D. A. Tennant, and S. E. Nagler, Phys. Rev. Lett. **85**, 832 (2000).

²² A. Zheludev, K. Kakurai, T. Masuda, K. Uchinokura, and K. Nakajima, Phys. Rev. Lett. **89**, 197205 (2002).

²³ F. H. L. Essler, A. M. Tsvelik, and G. Delfino, Phys. Rev. B **56**, 11001 (1997).

²⁴ A. Zheludev, S. Raymond, L.-P. Regnault, F. H. L. Essler, K. Kakurai, T. Masuda, and K. Uchinokura, Phys. Rev. B **67**, 134406 (2003).

²⁵ R. Coldea, S. M. Hayden, G. Aeppli, T. G. Perring, C. D. Frost, T. E. Mason, S.-W. Cheong, and Z. Fisk, Phys. Rev. Lett. **86**, 5377 (2001).